CI Cygni 2010 outburst and eclipse

Amateur spectroscopic survey

Christian Buil, Thierry Garrel, Benjamin Mauclaire, François Teyssier, Eric Sarrazin, Pierre Dubreuil
ARAS (Astronomical Ring for Acces to Spectroscopy)

First results from low resolution spectra

By François Teyssier
AAVSO and AFOEV member
Francois.teyssier@dbmail.com
03/01/2011

Presentation

The aim of this document is to present the amateur spectroscopic survey of the 2010 outburst of symbiotic star CI Cygni. This outburst coincides with an eclipse of the hot component by the late type giant star. After a review of the current knowledge of this system, the campaign is presented.

The firsts results obtained from low resolution spectra are described.

1. Introduction

Symbiotic stars are binary systems composed of a cool giant and a hot, luminous white dwarf, surrounded by a ionized nebula.
CI Cyg is a symbiotic star containing a cool giant of type M5.5III (Mürset & Schmidt 1999) and a compact star. CI Cyg is one of the very few symbiotic systems in which the giant fills or nearly fills its Roche lobe and shows ellipsoidal photometric variations in its light curve, especially in R and near-IR bands (Mikolajewska 2003).
The nature of the compact star is still controversial. Kenyon & al. (1991) argued that the compact star should be a main sequence star surrounded by an extended accretion disk. Godon (1996) derived T > 100 000 K as the temperature of the boundary layer of the disk. This high temperature allows the formation of high ionization emission lines (HeII, [Fe VII]) observed in CI Cyg during quiescent states. Godon's model shows that a large expansion in the radius of the accreting star explains the much lower temperature (T <= 20 000 K) observed during outbursts. The higher excitation lines thus vanish as the outburst progress. Tutukov & Yungelson proposed that a good fraction of symbiotic stars were powered by stable hydrogen nuclear burning on the surface of a white dwarf of the material accreted from the cool giant. The burning envelope would react with an expansion to any increase of the accretion rate. The expansion of the pseudo-photosphere cause its cooling. According to this model, the pseudo-photosphere would shift its energy peak from far UV to optical range, causing the star to appear in "outburst".

At quiescence, the spectrum is dominated by the molecular absorption bands of the cool giant star, Balmer, HeI and high ionization emission lines (HeII, [Fe VII]) powered by the very hot companion (fig. 1)

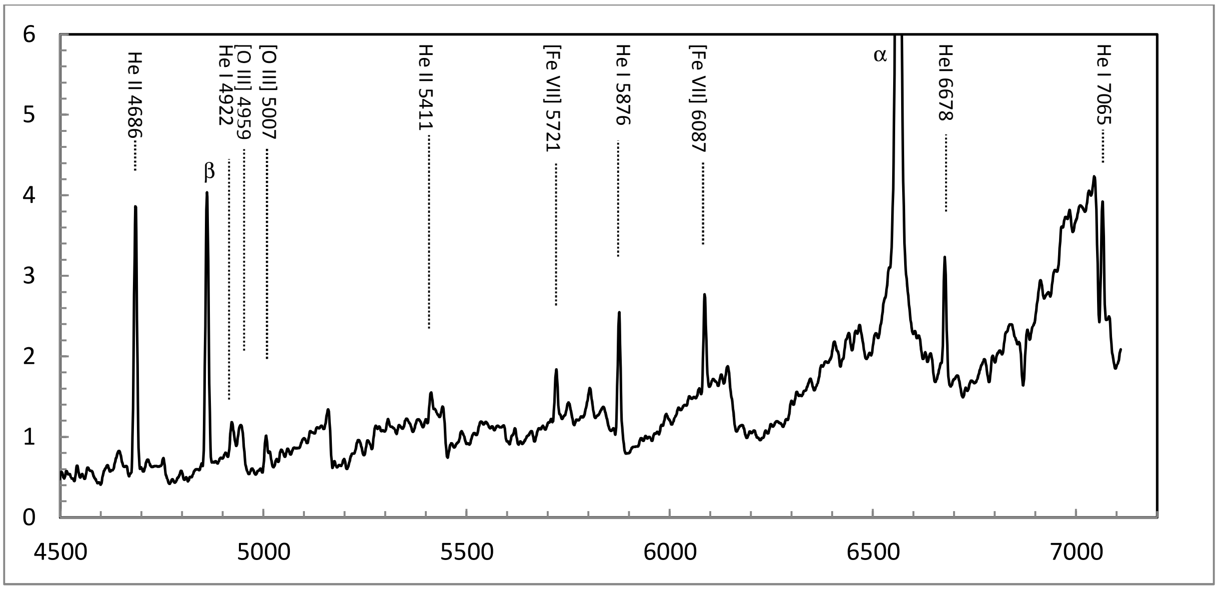

Fig. 1. CI Cygni spectrum at the beginning of the outburst (2010 June, 30). Hα line have been truncated in favor of fainter features

Eclipses have been detected in the light curve.
The permitted emission lines shows a pronounced eclipse effect. The lack of eclipse in forbidden emission lines suggests that they are emitted in a much larger region than Balmer and Helium lines (Mikolajewka, 1985)

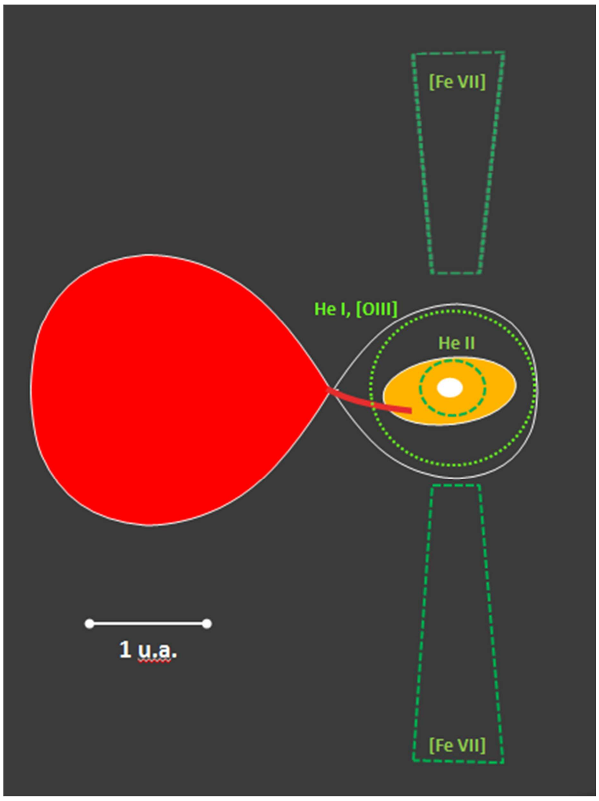

Fig. 2 – A schematic representation of CI Cyg adapted from Kenyon & al. (1991).
The M giant fills its Roche lobe and transfer material into an extended disk surrounding the hot component. The disk is surrounded by a small He II region and a larger HeI, [OIII] zone. A larger highly ionized region ([FeVII],[NeIII]) a been detected by eclipses studies, but its geometry remains uncertain.

This system shows classical symbiotic outbursts. Those of 1911 and 1937 have been minor ones in brightness amplitude and duration. Between 1970 and 1978, CI Cyg has undergone an active phase consisting of several optical brightenings with amplitude up to 2 mags, with three maxima occurring on Nov 1971, Nov 1973 and Aug 1975. A sharp minimum, centered on Oct 4, 1975 was caused by a total eclipse of the outbursting component by the giant star. (Fig. 3) After a long quiescence state, lasting for 3 decades, a new series of outbursts has begun in 2008 (AAVSO Special Notice #121)

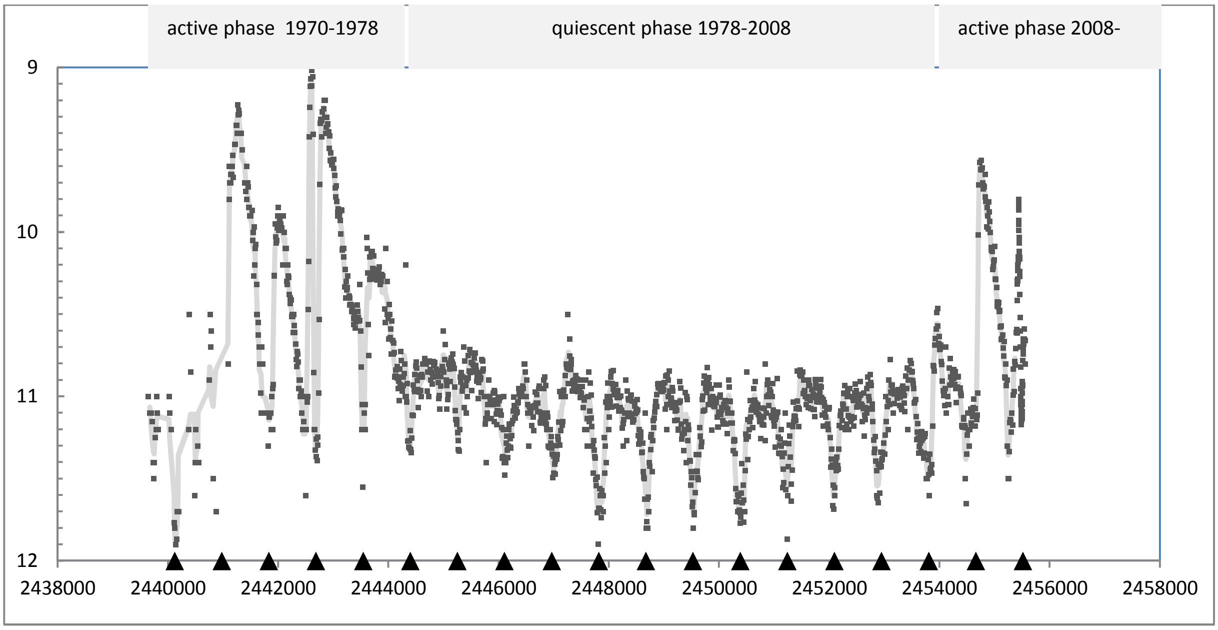

Fig 3. Long term light curve (Visual and CCD V 10-days mean) from AAVSO observers. Eclipses are marked by triangles.

The 2010 outburst has first been detected by Munari & al (2010). This outburst coincides with an eclipse of the hot component.

2. Observations

High and low resolution spectra were acquired by several amateurs in France.
The fit and dat files can be downloaded from : http://www.astrosurf.com/aras/CICyg/CI_Cyg.html
From june 30 to December 25, 68 spectra have been acquired, in low and high resolutions :

High resolution

Observer	Telescope	Spectrograph	Resolution	Approximate Range	Number of spectra
Christian BUIL	SC 28cm	eShel	11 000	428-712 nm	16
Thierry GARREL	SC 21 cm	LHIRES III 2400 l/mm	15 000	650-661 nm	13
Benjamin MAUCLAIRE	SC 21 cm	LHIRES III 2400 l/mm	15 000	652-669 nm	4

Low resolution

Observer	Telescope	Spectrograph	Resolution	Approximate Range	Number of spectra
Christian BUIL	SC 23 cm	LISA 300 l/mm	1000	390-730 nm	1
François TEYSSIER	SC 25 cm	LHIRES III 150 l/mm	800	440-720 nm	34

A few spectra have also been acquired using a slitness 100l/mm spectrograph (StarAnalyser) by Eric Sarrazin and Pierre Dubreuil.

All spectrographs (eShel, Lhires, Lisa, StarAnalyser) are Shelyak Instruments products.

Fig. 4 - Some samples of spectra at different resolutions

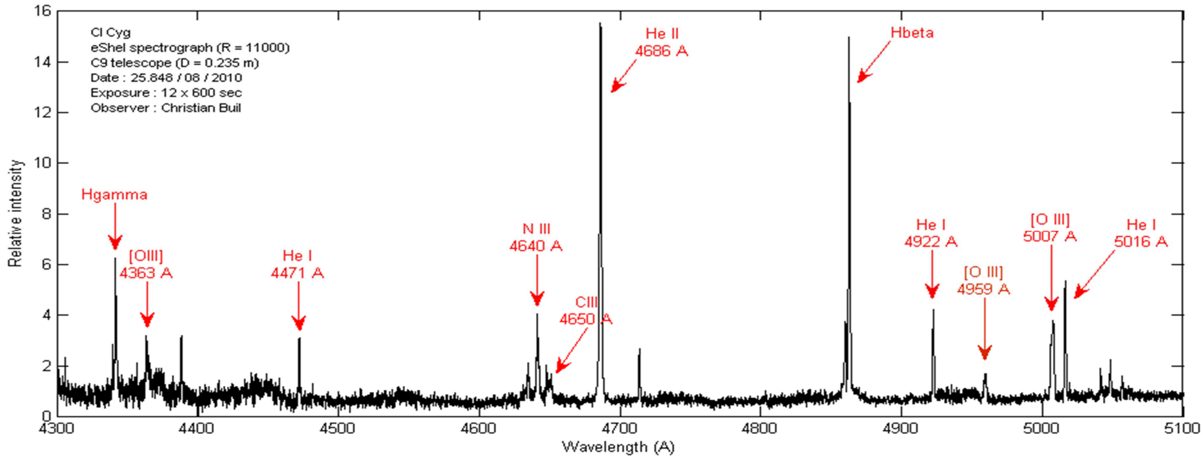

Fig. 4-1 - A part of eShel spectrum (R = 11000), with line identification by Christian Buil

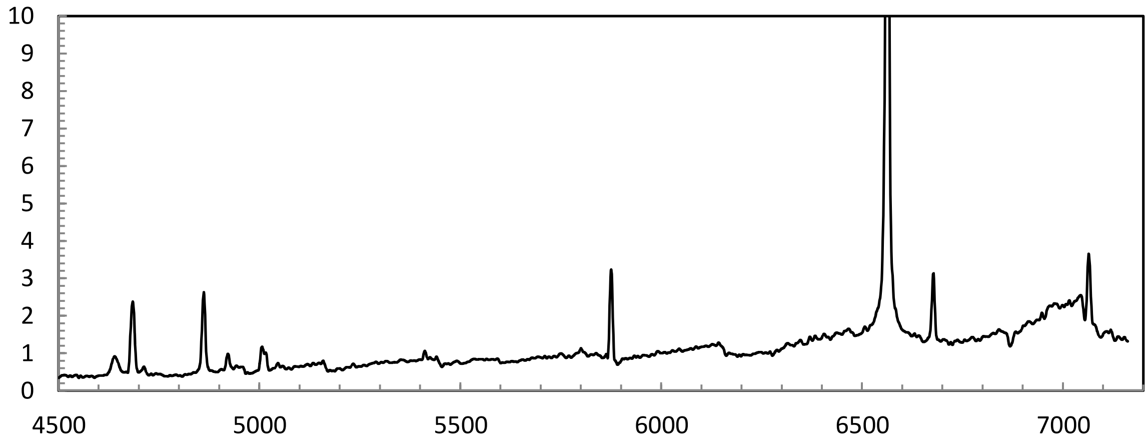

Fig 4-2 -Low resolution (R = 800) by François Teyssier

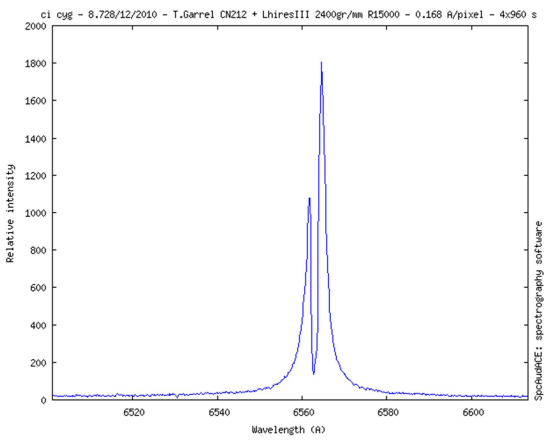

Fig. 4-3 - High resolution spectrum of Hα line (R = 15000) by Thierry Garrel

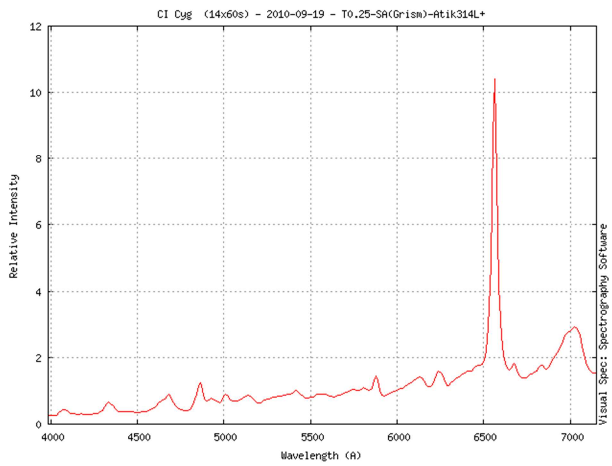

Fig. 4-4 – Very low resolution (slitness StarAnalyser) by Eric Sarrazin

3. Luminosity curve from AAVSO data

The photometric evolution of CI Cygni is presented in Fig. 6. Up to July 20th, 5-days means visual data are used (dotted line). The solid line shows the daily-mean CCD V data since July 20th.

The luminosity increases irregularly during about 3 months from Vis = 11.2 to a maximum V = 9.8 (Aug 26th) with a mean increase of -0.013 mag.d^{-1}. This rate shows significant accelerations especially between July 22 and 31th and between August 16th and 26th with respectively -0.032 and - 0.036 mag.d^{-1} rates.

The eclipse begins on August 26th (JD 2455435) and ends on November 14th (JD 2455515) with a total duration of 80 days. This is much less than the 1975 eclipse duration established at 130 days (Mikolajewska, 1983). The eclipse ingress is quiet linear with minor variations in the slope, with a mean value of 0.035 mag.d^{-1} . During the totality, the profile shows a U shape (from September 29th to October 26th – JD 2455469 to 2455496) and was going throw the minimum on October 14th (JD 2455484) at V = 11.16. The totality duration is 30 days, also much less than during 1975 (72 days estimated by Miko 1983)

The eclipse egress lasts 16 days, with a mean rate of 0.019 mag.d^{-1} and ends at V ~ 11.7. The luminosity is almost stable since eclipse ends.

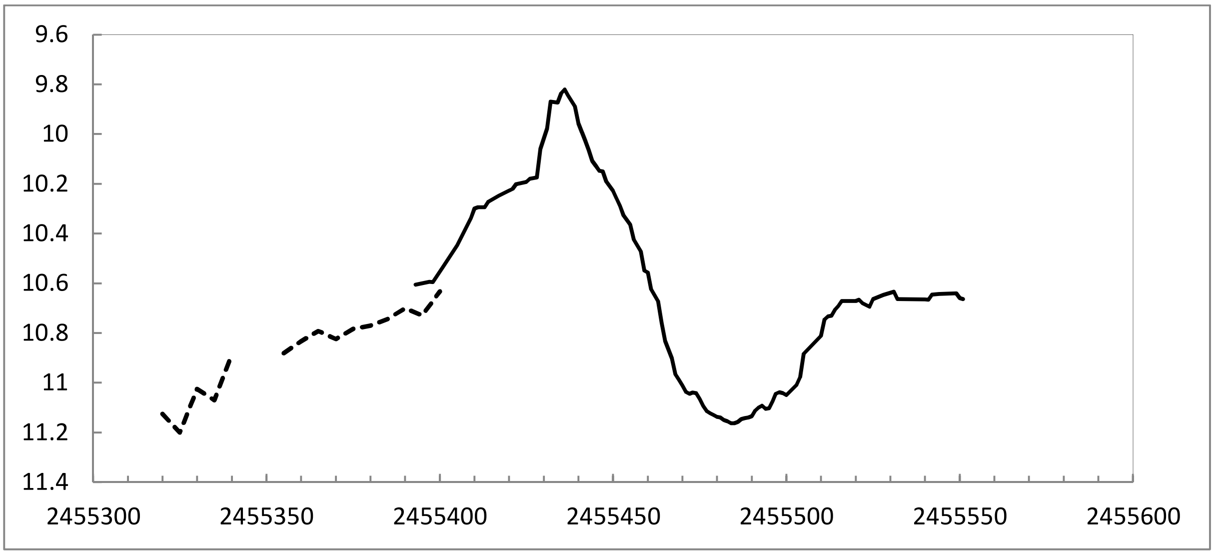

Fig. 5 – Visual (dotted line) and CCD V (solid line) light curve from AAVSO data.

The comparison of profiles (Fig. 6) shows that the 2010 outburst is much more shorter than 2008-2009 and 1975 ones.

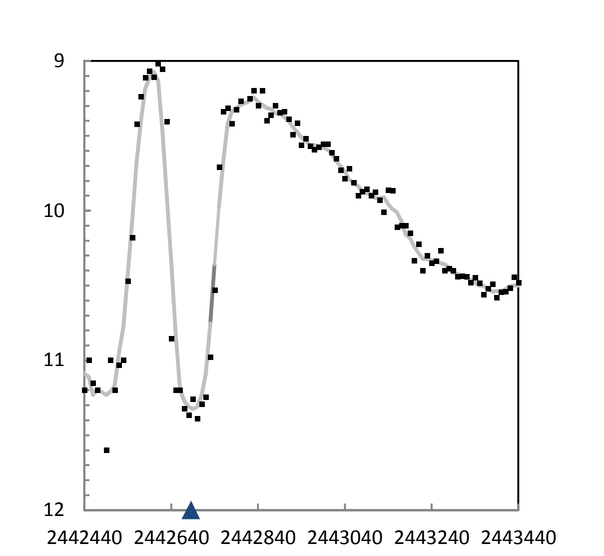

Fig. 6-1 1975 outburst and eclipse

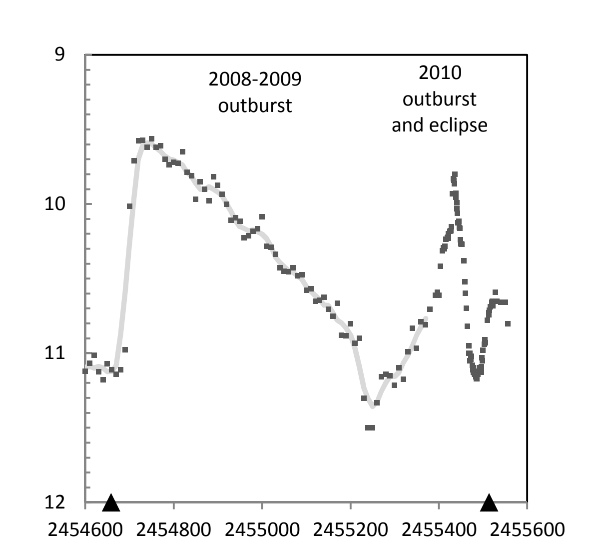

Fig. 6-2 2008-2010 outbursts and 2010 eclipse

Fig. 6 – comparison of 1975 and 2010 outbursts and eclipses photometric profiles

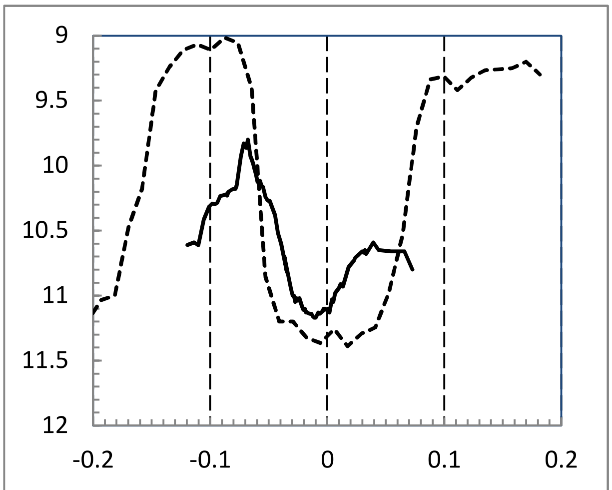

The 1975 and 2010 eclipse profiles have been plotted according to phase computed with the following ephemeris: Min(V) = 2 442 690 + 853.8E, where the epoch is the photocentre of the 1975 eclipse and the period is adopted from Frekel (2000).

The minimum luminosity occurs at phase = -0.02, i.e. 18 days before the minimum predicted by the spectroscopic ephemeris.

The profile is narrower than 1975 eclipse and less symmetric.

Fig. 7 - 1975 (dotted line) and 2010 (solid line) eclipse profiles according to phase.

4. Spectral evolution

The spectra were reduced with standard procedures, including the use of a standard star observation to correct for the wavelength dependent spectral response.

The spectral evolution is described in fig. 8 and 9

From june 30th to august 23th, the outburst progresses. The spectral variation shows the dramatic vanishing of high excitation lines, especially [FeVII]. The molecular absorption bands strongly weaken; they are partially filled by the emission from the hot components (Fig. 8-1)

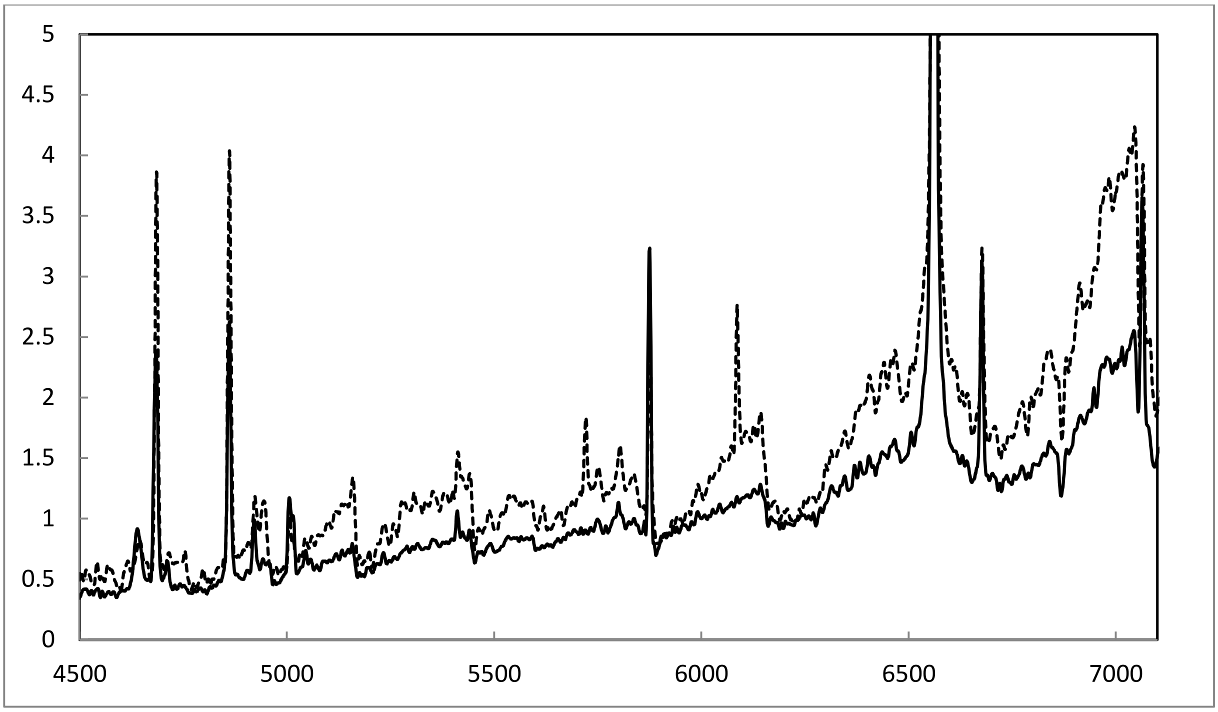

Fig. 8-1 – Spectral evolution between June 30th (dotted line) and August 24th (solid line)

From August 24th (while eclipse begins and outburst still progresses), to October 14th (at mid-eclipse) the absorption bands strengthen. At mid eclipse, the continuum is quite the same as at the beginning of the outburst. [FeVII] reappear slightly which shows the decline of outburst.

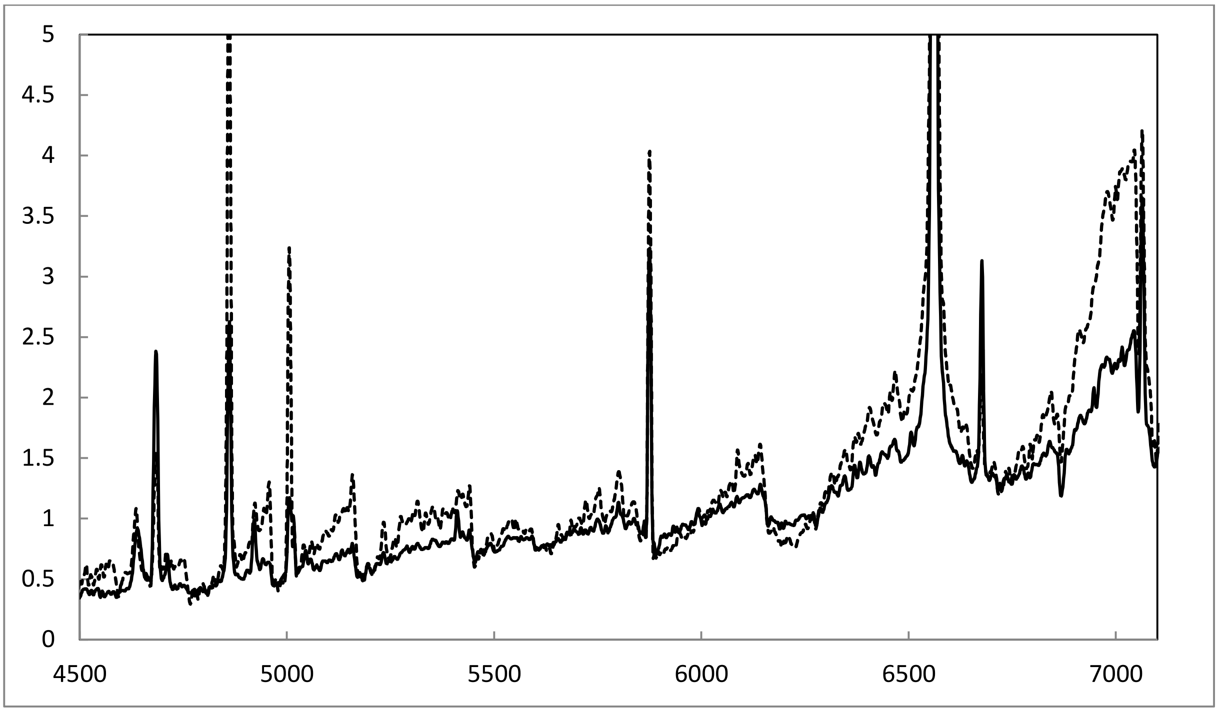

Fig. 8-2– Spectral evolution between and August 24th (solid line) and October 14th (dotted line)

The complete evolution is described by fig. 9 in which spectra are absolute fluxed.

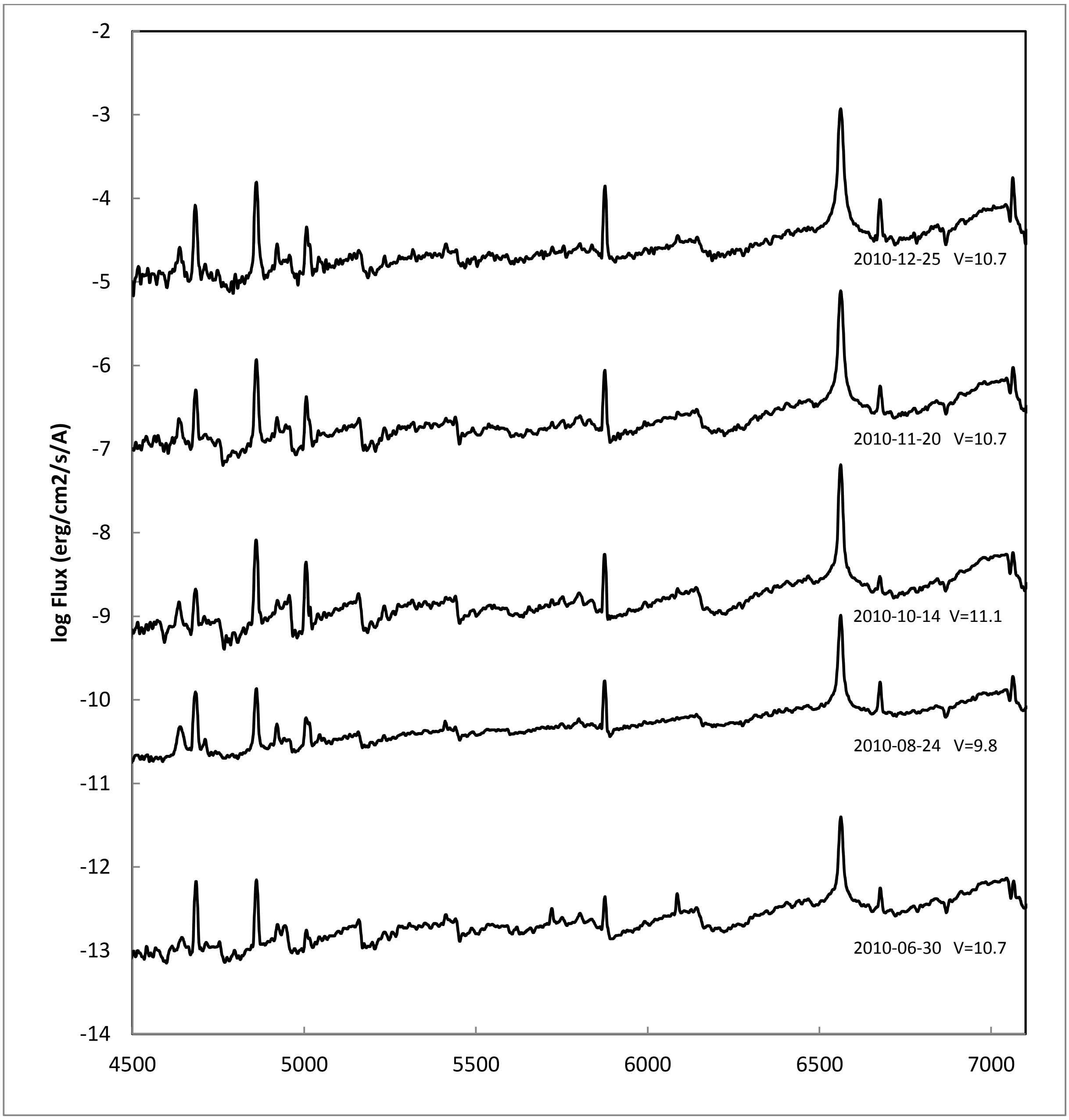

Fig. 9. Absolute flux spectral evolution of CI Cyg during the 2010 outburst. For clarity, the spectra are offset in ordinates by 2 units

5. Equivalent width variations

Equivalent widths have been measured on Hα, Hβ, HeI, HeII, [OIII] lines. Hα EW is directly measured. For the other lines, a Gaussian fitting is used. That permits notably to deblend the [OIII]/HeI lines.

Hα equivalent width has monotonically increased from june 30^{th} to august 18^{th}; a sudden decrease of 13% which coincide with a luminosity burst. The monotonic increase regain up to October 20^{th} .
At that time, a new sudden decrease of 14% is detected, 8 days after eclipse maximum. Since 20^{th} October EW Hα increases again monotonically. This evolution is plotted in fig. 9-1 where squares are

low spectra measures and crosses are measures obtained from eShel spectra obtained by Christian Buil.

The general shape of Hβ EW is similar to Hα EW one, with the two decreases observed in Ha EW curve.

HeII EW curve is completely different. The light curve and EW HeII looks remarkably similar. HeII is the only line whose EW evolution is clearly correlated with photometric curve during the eclipse phase.

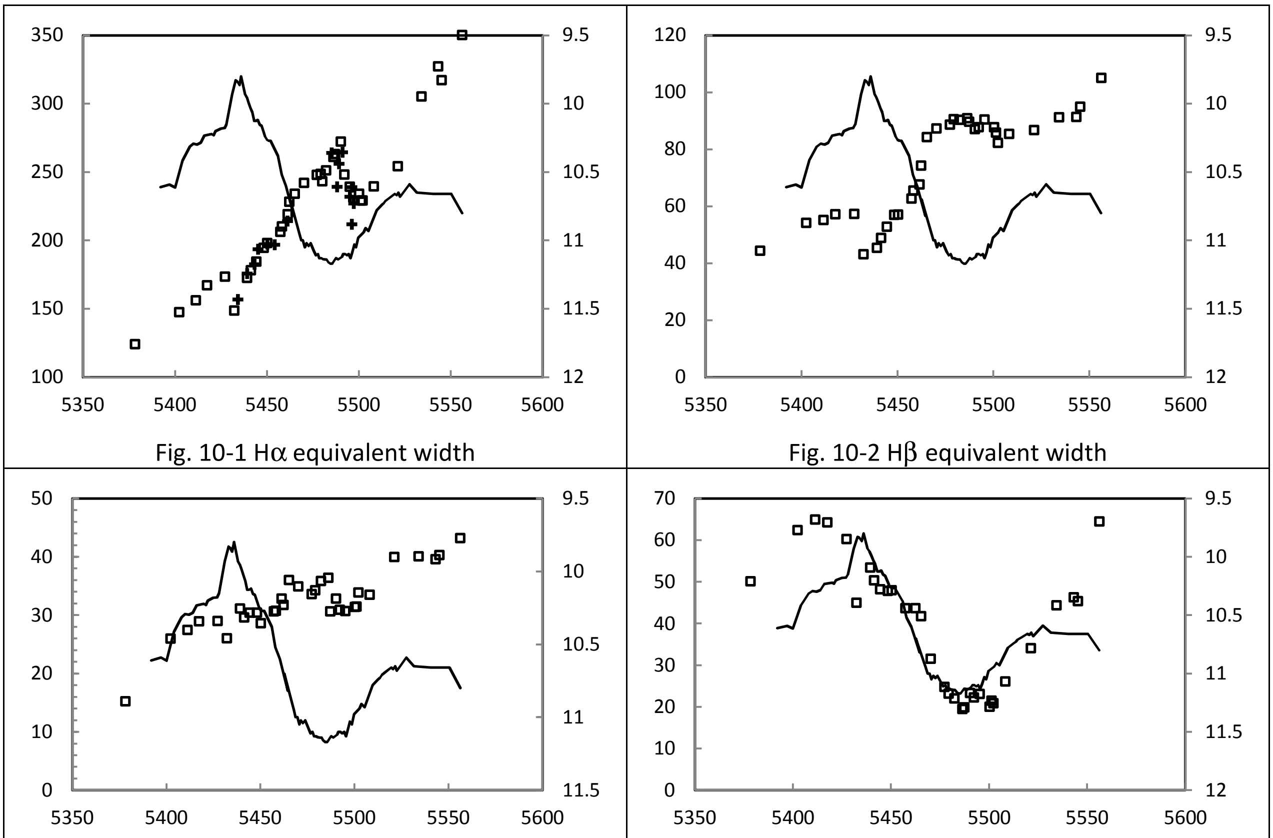

Fig. 10-1 Hα equivalent width

Fig. 10-2 Hβ equivalent width

Fig. 10-3 HeI λ 5876 equivalent width

Fig. 10-4 HeII λ 4686 equivalent width

Fig. 10 – Equivalent widths time series (JD-2450000). Squares for low resolution measures, crosses for eShel measures (only Hα)

The [OIII]/He I ratio (Fig. 11) has been almost stable up to mid-September (~ 15th), varying from 1.5 to 1.9. It then increases suddenly to a maximum value of 12.6 on JD 245586, October 16th, at phase -0.009, eight days before the predicted date.

The ratio decrease is also nearly linear, with a greater slope (+40% in comparison to the raising slope), to a minimum of 2.6, slightly greater than the one before eclipse.

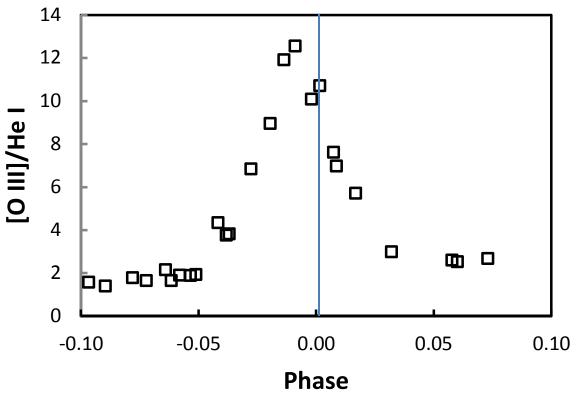

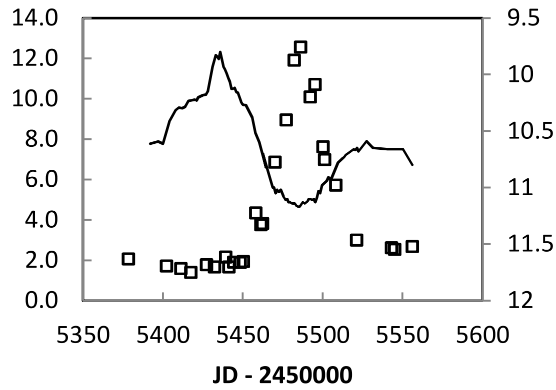

Fig. 11-1 [OIII]/HeI 5016 EW ratio vs phase	Fig. 11-1 [OIII]/HeI 5016 EW ratio vs JD – CCD V lightcurve : solid line

Fig. 11 – [OIII]/HeI ratio vs phase

6. Absolute flux lines variations

Absolute flux calibration has been obtained by scaling the continuum by the CCD V magnitude in the range 530-582 nm (O'Connell 1973). The conversion V mag to absolute flux has been computed by the Spitzer Science Center Magnitude to Flux Density Converter which overestimates the result by a factor 1.05 in comparison to the classical formula log F_λ = -0.400V-8.449 erg.s^{-1}.cm^{-2}.Å^{-1}

HI, HeI and HeII absolute flux and luminosity curves looks remarkably similar, unless they go on increasing after eclipse ends while the V mag is almost stable (fig. 9).
All these lines show pronounced eclipse effects. The amplitude of these eclipse vary from about twice for HI lines up to 6 for HeII λ 4686 (3 for He I λ 5876). These values are similar to those estimated during 1975 eclipse (Mikolajewka and Mikolajewski, 1983)

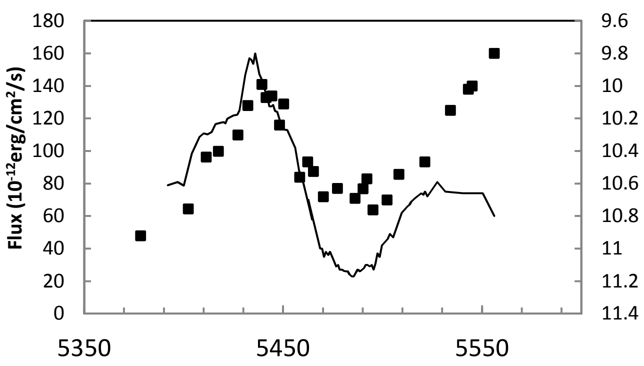

Fig. 12-1 Hα absolute flux

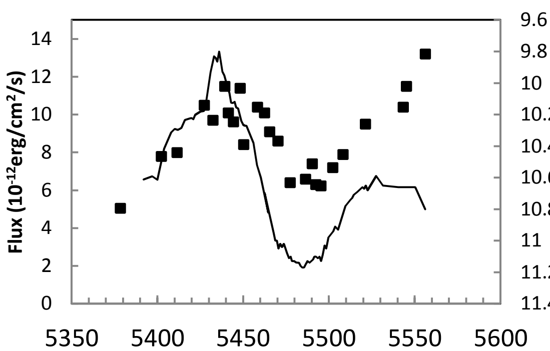

Fig. 12-2 Hβ absolute flux

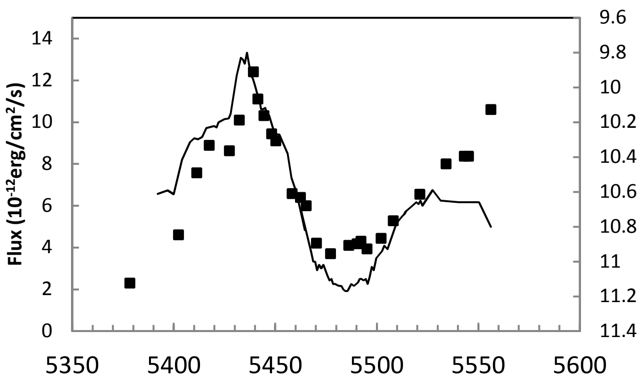

Fig. 12-3 HeI λ 5876 absolute flux

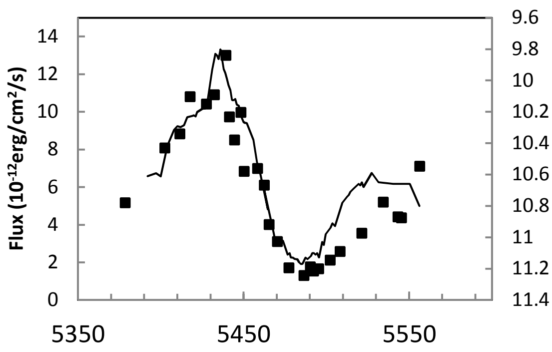

Fig. 12-4 HeII λ 4686 absolute flux

Fig.12– Absolute line flux (erg.s^{-1}.cm^{-2}.$Å^{-1}$) vs time (JD-2450000) and CCD light curve (right scale)

[OIII] λ 5007 flux measurements are more scattered. There's no detectable eclipse effect. The [OIII] emission region is more extended than HI, HeI and HeII zone (Mikolajewska & Mikolajewski 1983). The maximum intensity is detected on about September 25th (JD 2455465). This could be a good indication of outburst maximum, about at the mid ingress phase.

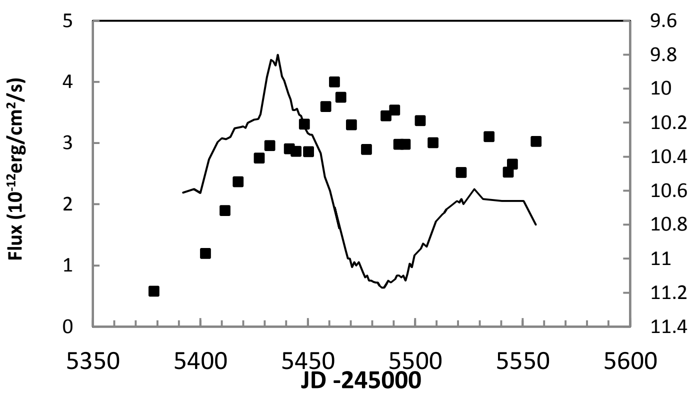

Fig. 13 [OIII] λ 5007 absolute flux evolution

7. Continuum variations

At the beginning of the outburst (30th june) the continuum matches correctly with a M5III standard star, HD 221615, from The Indo-U.S. Library of Coudé Feed Stellar Spectra (Fig 13-1).

When outburst progresses the absorption bands are reduced. At maximum luminosity the continuum doesn't match with any earlier spectral type continuum (M3 or M4). A synthetic spectrum has been computed consisting of a M5III spectrum and a HI recombination continuum at T = 5000 K. (Fig 13-2).

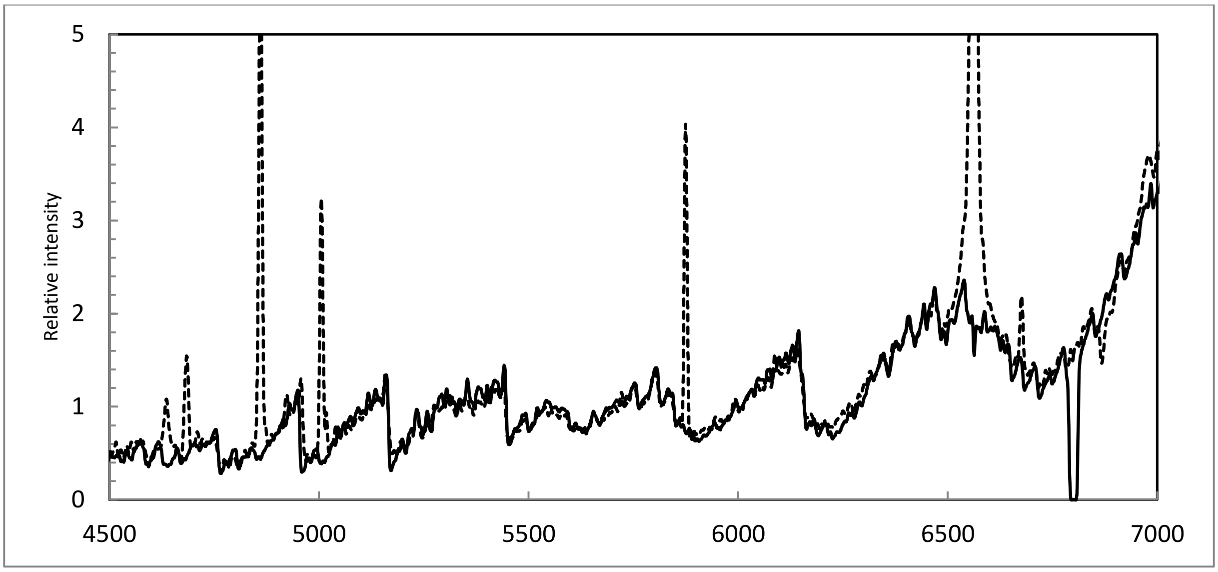

Fig 13-1. Comparison between the June 30th spectrum (dotted line) and a M5III standart

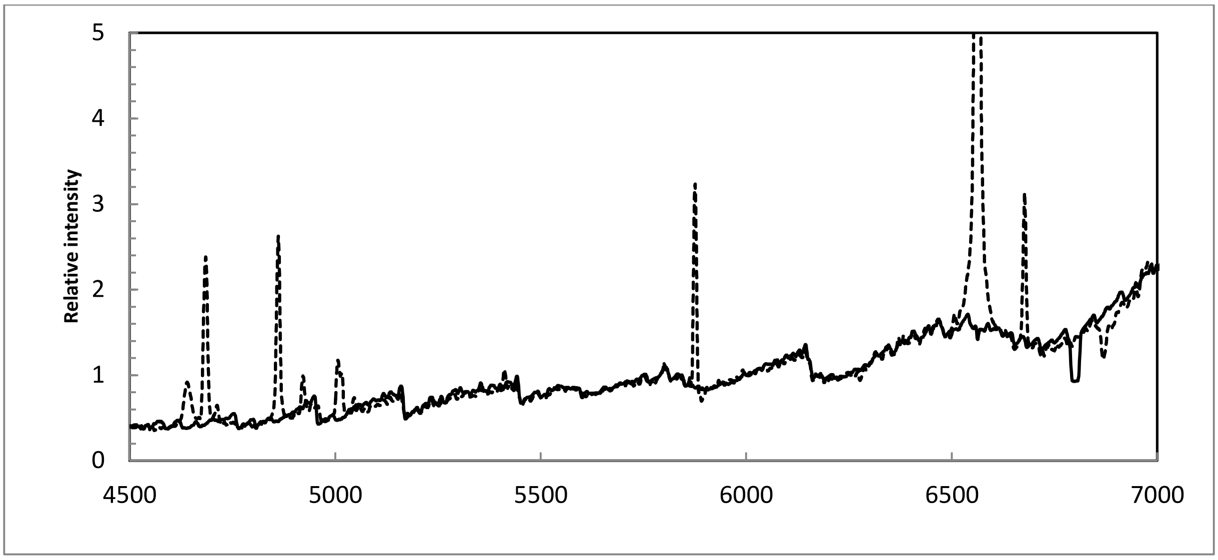

Fig. 13-2 At max luminosity (August 24th), the continuum matches with a synthetic spectrum : M5III composite with a HI recombinaison continuum (T = 5000 K).

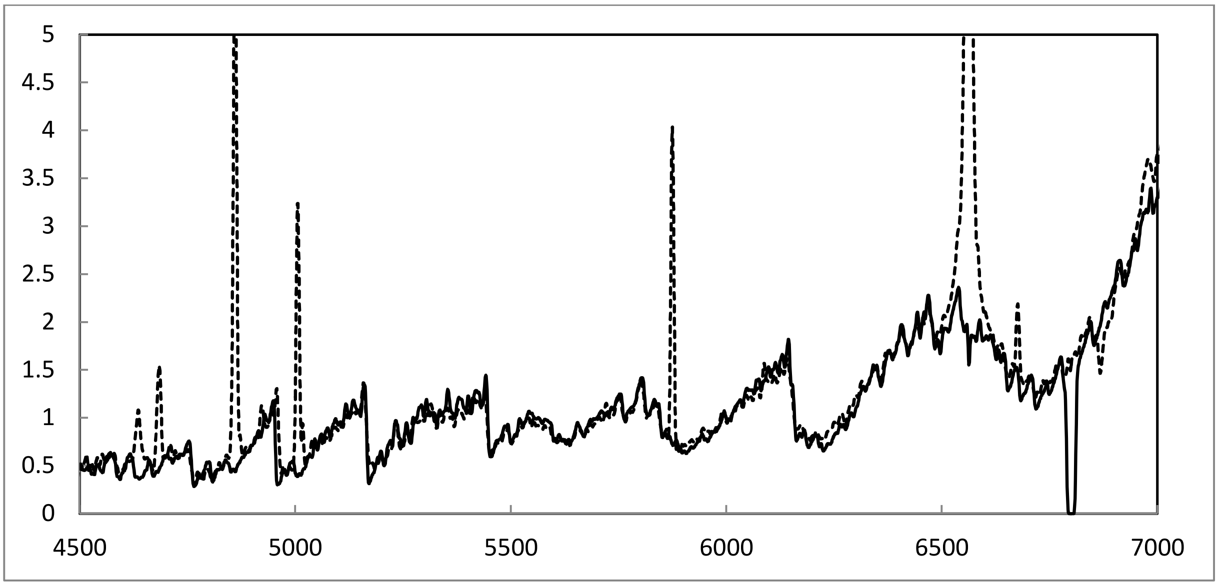

Fig 13-3 At mi-eclipse, the continuum matches again with a M5 III standard

Fig. 13 - CI Cygni spectra : dotted lines – Comparison spectra : solid lines.

The continuum variations have been measured with two TiO indices as defined by Kenyon and Fernandez Castro (1987).
TiO1 measures the 6125 Å TiO band while TiO2 measures 7025 6125 Å TiO band.

As illustrated in Fig. 14, the two TiO indices are strongly correlated with luminosity V curve.

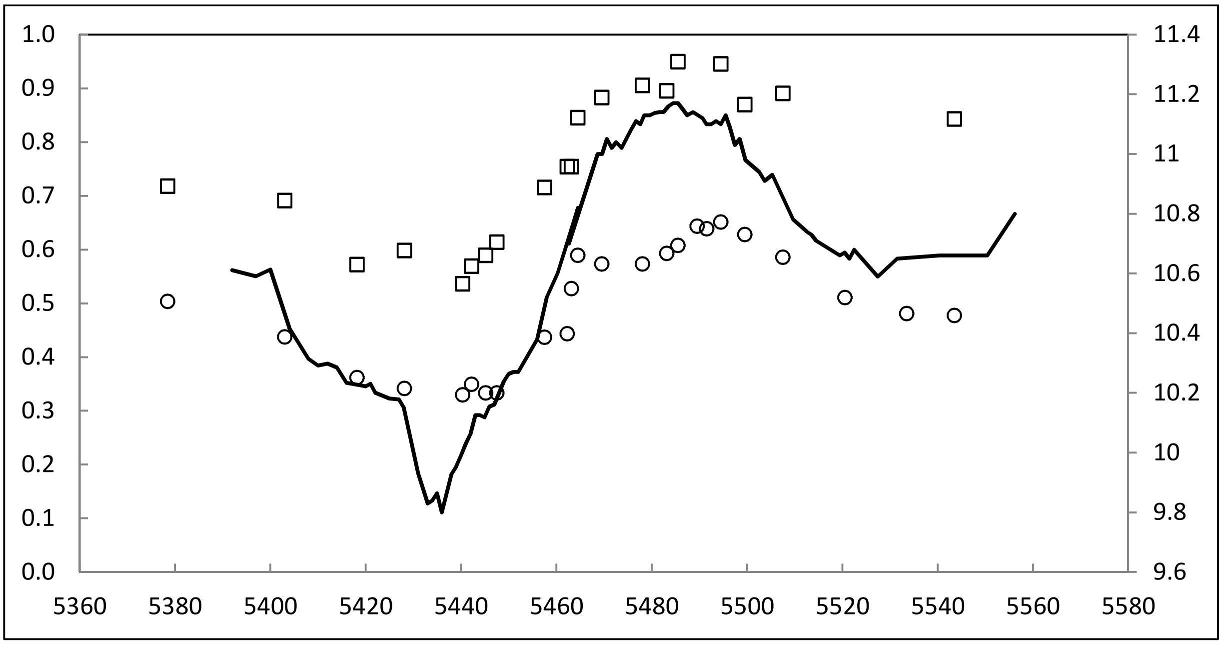

Fig. 14 – TiO indices variation vs JD (-2450000) and V magnitude (solid line)
TiO 1 : squares – TiO 2 : circles

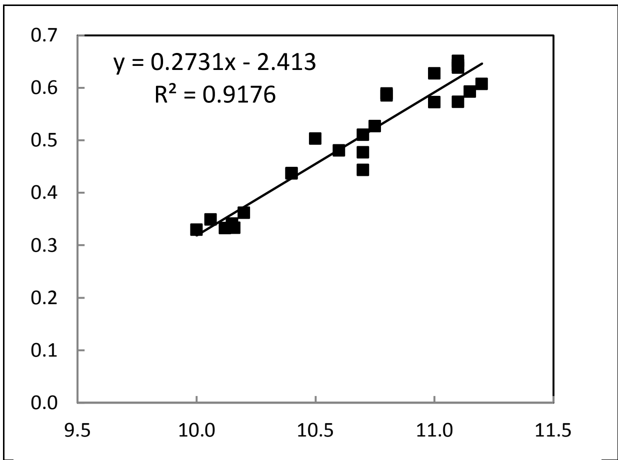

Fig 15-1 TiO1 indice vs V magnitude

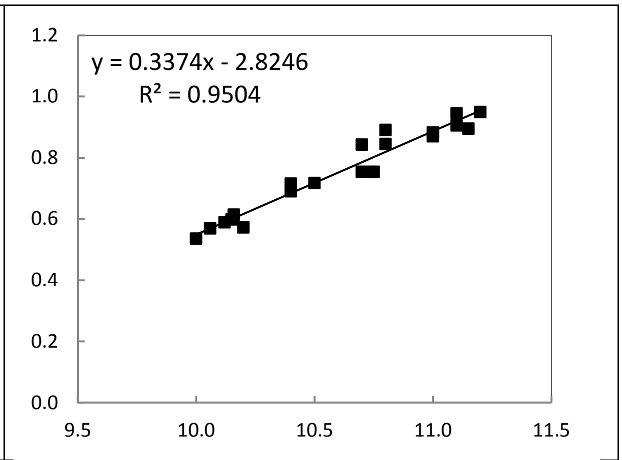

Fig. 15-2 TiO2 indice vs V Magnitude

The correlation is illustrated by graphs showing TiO indices vs V magnitude, with strong coefficients.

Acknowledgements

I would like to thank the AAVSO visual and CCD observers who acquired the photometric data used in this document and especially for CCD measurements :
I gratefully acknowledge Dr Michael Friedjung (IAP) for his very helpful advices.

References

AAVSO Special Notice #121, Outburst of the symbiotic star CI Cygni, August 31, 2008

Frekel, F.C., Joyce, R.R., Hinkle, K.H., Skrutskie, M. F.,AJ, **119**, 2000

Kenyon, S.J., Fernandez Castro, T., 1987, AJ, **93,** 1987

Kenyon, S. J., Oliversen, N. A., Mikolajewska, J., Mikolajewski, M., Stencel, R. E., Garcia, M. R., Anderson, C. M., A.J., **101**, 1991

Munari U., Siviero A., Cherini G., Dallaporta S., Valisa P.**, ATel #2732,** 12 Jul 2010

Mikolajewsja J., Mikolajewski M., Acta Astronomica, **33**, 1983

ANNEXES

#	Date	JD - 2450000	Phase	Ha	Hb	HeII λ 4686 Å	HeI l5876	[OIII]/HeI
1	30/06/2010	5378.417	-0.135	124	44.2	50.2	15.2	2.1
2	24/07/2010	5402.393	-0.107	147	54.0	62.4	26.0	1.7
3	02/08/2010	5411.403	-0.097	156	55.1	65.0	27.4	1.6
3	09/08/2010	5417.534	-0.090	167	57.1	64.3	28.9	1.4
4	18/08/2010	5427.390	-0.078	173	57.2	60.3	29.0	1.8
5	23/08/2010	5432.330	-0.072	149	43.0	45.0	26.1	1.7
6	30/08/2010	5439.333	-0.064	172	45.3	53.5	31.2	2.2
7	01/09/2010	5441.426	-0.062	178	48.7	50.4	29.6	1.7
8	04/09/2010	5444.440	-0.058	184	52.7	48.2	30.4	1.9
9	08/09/2010	5448.330	-0.054	194	56.9	47.8	30.4	1.9
10	10/09/2010	5450.335	-0.051	198	57.0	48.0	28.6	1.9
11	17/09/2010	5457.383	-0.043	206	62.6	43.6	30.6	
12	18/09/2010	5458.325	-0.042	210	65.4		30.8	4.3
13	21/09/2010	5461.396	-0.038	219	67.5		32.9	3.8
14	22/09/2010	5462.389	-0.037	228	74.1	43.7	31.8	3.8
15	25/09/2010	5465.360	-0.034	234	84.1	41.8	36.0	
16	30/09/2010	5470.300	-0.028	242	87.2	31.6	34.9	6.8
17	07/10/2010	5477.325	-0.020	248	88.5	24.8	33.6	8.9
18	09/10/2010	5479.317	-0.017	248	90.5	23.2	34.3	
19	10/10/2010	5480.300	-0.016	243				
20	12/10/2010	5482.325	-0.014	251	90.3	22.0	35.8	11.9
21	16/10/2010	5486.316	-0.009	261	90.8	19.5	36.4	12.6
22	17/10/2010	5487.301	-0.008	263	89.6	19.9	30.6	
23	20/10/2010	5490.309	-0.004	272	87.0	23.3	32.9	
24	22/10/2010	5492.278	-0.002	248	87.7	22.2	30.9	10.1
25	25/10/2010	5495.271	0.001	239	90.3	23.1	30.7	10.7
26	30/10/2010	5500.291	0.007	234	87.7	20.0	31.4	7.6
27	31/10/2010	5501.285	0.009	229	85.7	21.5	31.5	7.0
28	01/11/2010	5502.275	0.010	229	82.1	20.9	33.9	
29	07/11/2010	5508.244	0.017	239	85.3	26.1	33.5	5.7
30	20/11/2010	5521.273	0.032	254	86.6	34.1	40.0	3.0
31	03/12/2010	5534.290	0.047	305	91.1	44.4	40.1	
32	12/12/2010	5543.252	0.058	327	91.3	46.3	39.6	2.6
34	14/12/2010	5545.213	0.060	317	94.9	45.4	40.3	2.5
35	25/12/2010	5556.250	0.073	350	105.0	64.5	43.2	2.7

Tab. 1 - Emission line equivalent width (Å)

#	date	JD -2450000	Phase	Hα	Hβ	HeI 5876 Å	HeII 4686 Å	[OIII] 5007 Å
1	30/06/2010	5457.417	-0.755	48	5.1	2.3	5.2	0.6
2	24/07/2010	5481.393	-0.609	65	7.8	4.6	8.1	1.2
3	02/08/2010	5490.403	-0.783	96	8.0	7.6	8.8	1.9
3	09/08/2010	5496.534	-0.097	100	0.0	8.9	10.8	2.4
4	18/08/2010	5506.390	-0.349	110	10.5	8.6	10.4	2.8
5	23/08/2010	5511.330	-0.962	128	9.7	10.1	10.9	3.0
6	30/08/2010	5518.333	-0.325	141	11.5	12.4	13.0	3.8
7	01/09/2010	5520.426	-0.043	133	10.1	11.1	9.7	2.8
8	04/09/2010	5523.440	-0.756	134	9.6	10.3	8.5	2.9
9	08/09/2010	5527.330	-0.514	116	11.4	9.4	10.0	3.4
10	10/09/2010	5529.335	-0.327	129	8.4	9.1	6.8	2.9
12	18/09/2010	5537.325	-0.614	84	10.4	6.6	7.0	3.6
14	22/09/2010	5541.389	-0.182	94	10.1	6.4	6.1	4.0
15	25/09/2010	5544.360	-0.942	88	9.1	6.0	4.0	3.8
16	30/09/2010	5549.300	-0.555	72	8.6	4.2	3.1	3.3
17	07/10/2010	5556.325	-0.894	77	6.4	3.7	1.7	2.9
21	16/10/2010	5565.316	-0.089	71	6.6	4.1	1.3	3.5
23	20/10/2010	5569.309	-0.735	77	7.4	4.2	1.8	3.5
24	22/10/2010	5571.278	-0.588	83	6.3	4.3	1.5	3.0
25	25/10/2010	5574.271	0.676	64	6.2	3.9	1.7	3.0
28	01/11/2010	5581.275	0.314	70	7.2	4.4	2.1	3.4
29	07/11/2010	5587.244	0.823	86	7.9	5.3	2.6	3.0
30	20/11/2010	5600.273	0.032	94	9.5	6.6	3.6	2.5
31	03/12/2010	5613.290	0.227	125	0.0	8.0	5.2	3.1
32	12/12/2010	5622.252	0.000	138	10.4	8.4	4.4	2.5
34	14/12/2010	5624.213	0.138	140	11.5	8.4	4.4	2.7
35	25/12/2010	5635.250	0.174	160	13.2	10.6	7.1	3.0

Tab. 2 - Emission line absolute flux (10^{-12} $erg.cm^{-2}.s^{-1}$)